

ANALYSIS AND EVALUATION OF THE INFLUENCE OF HEAT STORAGE MATERIAL ON COKE OVEN FLUE GAS EXOTHERMIC PROCESS

by

Yu-Jie ZHAO^a, Jun-Xiao FENG^{a,b*}, Shi-Ping HUANG^c, and Shou-Yong HU^d

^a School of Energy and Environmental Engineering,
University of Science and Technology Beijing, Beijing, China

^b Beijing Key Laboratory for Energy Conservation and Emission Reduction in Metallurgical Industry,
Beijing, China

^c Hegang Group Co., Ltd., Shijiazhuang, China

^d Coking Plant of Handan Iron and Steel Group, Handan, China

Original scientific paper

<https://doi.org/10.2298/TSCI190715446Z>

Sufficient heat storage and proper flue-gas outlet temperature were prerequisites for selective non-catalytic reduction denitrification in coke oven regenerators. This work performed an energy balance analysis on the established regenerator model to obtain a new thermal storage evaluation index – total thermal storage temperature. Furthermore, ten cases of thermal storage parameters were set to analyze the effects of thermal effusivity and thermal diffusivity on heat storage and transfer. The transient simulation results shown that the channel shape of the lattice brick limited the uniformity of fluid-solid heat transfer and temperature distribution during the 30 minutes commutation period, and the temperature window (1100~1300 K) suitable for selective non-catalytic reduction denitration slowly moved down. The increase of thermal effusivity led to the rise of heat storage and reduction of flue-gas outlet temperature. However, the transform in thermal diffusivity did not contribute substantially to the heat storage performance. Besides, the temperature-time-height equation obtained by fitting was used for predicting the suitable location of selective non-catalytic reduction denitration temperature. The total thermal storage temperature was positively correlated with the flue-gas outlet temperature and negatively correlated with the heat storage capacity. The total thermal storage temperature evaluated the effects of material properties on heat storage and flue gas outlet temperature.

Key words: *thermal storage performance, total thermal storage temperature, selective non-catalytic reduction denitrification, coke oven regenerator*

Introduction

Coke oven flue gas NO_x emission has caused severe pollution the environment and society [1]. In recent years, the environmental protection department in China has issued a series of coking enterprises NO_x emission control policies. Especially for the coking plant in the Beijing-Tianjin-Hebei region, it is required that the NO_x emission of the newly built coking plants should not exceed 150 mg/m³ [2, 3].

* Corresponding author, e-mail: jxfeng@ustb.edu.cn

Most coking plants adopt the mature selective catalytic reduction (SCR) denitrification technology to meet strict environmental requirements. The SCR catalysts are widely applied into flue-gas denitration at temperatures ranging from 310–400 °C in thermal power plants [4]. For coke oven flue-gas with complex composition and low temperature, direct use of SCR denitration achieve NO_x emission reduction has significant obstacles. Some enterprises adopt the technical route of coke oven flue-gas preheating before denitrification, viz., a heating furnace is set before coke oven flue-gas enters SCR denitrificationwer to raise the temperature of flue-gas, to reach the optimal SCR denitrification temperature. Although this technology route significantly reduces NO_x emissions, the secondary heating of flue-gas will undoubtedly result in increased energy consumption and cost. Yu *et al.* [5, 6] studied that the working temperature of the low temperature catalyst was 200–300 °C, and the denitrification rate could reach 80%. The application of low temperature catalyst in coke oven flue-gas denitrification efficiency can effectively reduce energy consumption without additional energy consumption and equipment input. Even so, the SCR denitrification system added to the coke oven system adds a lot of equipment, which requires enormous investment and operation costs, making the enterprise unbearable.

In addition to the previous, much attention has been paid to the control of NO_x emission reduction in coke oven combustion. Buczynski *et al.* [7] calculated that the heat recovery coke oven under negative pressure operation indicated that the number of harmful gases emitted by the environment was relatively low. Jin *et al.* [8], Belašević *et al.* [9], and Hodzic *et al.* [10] simulated the large-capacity coke oven staged combustion improve the temperature uniformity of the coke bed and reduce the NO_x emission concentration. Gamrat *et al.* [11] introduced the external flue gas circulation rate of 0.2 and NO_x emission reduction of 50%. The control method of NO_x in the combustion process flue-gas only reduces the content of NO_x in the flue gas, but it is still unable to meet the environmental protection requirements.

Selective non-catalytic reduction (SNCR) denitrification technology, which is also widely used as well as SCR denitrification, can reduce NO_x to N₂ without catalyst by mixing reducing agent such as ammonia or urea with the high temperature flue gas (800–1100 °C). SNCR technology is suitable for flue gas with complex high temperature components. It has the characteristics of a simple system, less investment and small running resistance, so it is widely used in cement, ceramics, waste incineration and other fields. Some coking enterprises put forward an integrated method of spraying ammonia on the top of the combustion chamber or the top of the regenerator [12, 13]. The technique utilizes the heat energy of the coke oven high temperature flue gas to combine the waste heat step utilization with the SNCR denitrification, thereby avoiding the input of the hot blast stove and the denitration equipment, saving energy consumption and reducing the denitration cost. However, due to the complex composition of the coke oven flue gas, temperature fluctuation and the excessive temperature of the SNCR ammonia injection position, the NO_x emission reduction effect was weak, and the ammonia escape was increased.

This paper aims to select the suitable position of ammonia injection in the *Y*-direction of the regenerator without affecting the sufficient regeneration of the coke oven and the outlet temperature of the flue gas. The method of increasing the heat storage capacity of the regenerator is adopted to reduce the occupied space of solid heat storage materials and leave enough space for ammonia injection, furthermore, make the flue gas and reducing agent mix sufficiently. Also, the total thermal storage temperature (TTST) is proposed as an evaluation index of heat storage to measure the influence of material physical properties on heat storage and flue gas outlet temperature. It is expected that this study can predict the temperature and

position changes of SNCR denitrification and evaluate the thermal storage performance of coke oven with changed materials.

Evaluating method

Evaluation scheme design

The heat storage capacity of coke oven regenerator mainly depended on the specific heat capacity and density of solid heat storage material. Volume heat capacity of unsteady heat storage process was also related to the thermal conductivity. This paper mainly selected three essential parameters of solid material, namely specific heat, density, and the thermal conductivity, and designed the evaluation scheme of solid material parameters for heat storage, tab. 1. Based on Case 1, the initial values of specific heat c_0 , density ρ_0 , and thermal conductivity λ_0 were, respectively, set as 1075 J/kgK, 1900 kg/m³, and 1.2772 W/mK.

Table 1. The evaluation design scheme for parameter of heat storage materials

Case number	Specific heat [Jkg ⁻¹ K ⁻¹]	Density [kgm ⁻³]	Thermal conductivity [Wm ⁻¹ K ⁻¹]
Case 1	c_0	ρ_0	λ_0
Case 2	$c_0 + 100$	ρ_0	λ_0
Case 3	$c_0 + 200$	ρ_0	λ_0
Case 4	$c_0 + 300$	ρ_0	λ_0
Case 5	c_0	$\rho_0 + 100$	λ_0
Case 6	c_0	$\rho_0 + 200$	λ_0
Case 7	c_0	$\rho_0 + 300$	λ_0
Case 8	c_0	ρ_0	$\lambda_0 + 1$
Case 9	c_0	ρ_0	$\lambda_0 + 2$
Case 10	c_0	ρ_0	$\lambda_0 + 3$

Evaluation index

Coke oven regenerator periodically absorbs the heat of high temperature flue gas. To ensure that the coke oven chimney should always be *hot-standby*, the temperature of flue gas discharged from the chimney should be guaranteed to be greater than 140 °C [14], and the outlet temperature of the bottom of the lattice brick should not exceed 350 °C. Therefore, the coke oven regenerator stored a large amount of heat, but it was also limited by the regeneration time and the flue-gas outlet temperature. Three indexes were proposed to evaluate the influence of different heat storage materials to satisfy the coupling of heat storage and SNCR denitrification.

Thermal effusivity

The thermal effusivity [15] includes the main thermal parameters of solid thermal storage materials, which characterizes the ability to exchange heat energy with the surrounding environment. The thermal effusivity is given:

$$\kappa = (\lambda\rho c)^{1/2} \quad (1)$$

where κ [Ws^{0.5}m⁻²K⁻¹] is the thermal effusivity, λ – the thermal conductivity, ρ – the density, and c – the specific heat.

Thermal diffusivity

The thermal diffusivity [16] is an indicator of the ability of a material to propagate temperature changes within itself. In eq. (2), θ [m^2s^{-1}] is the thermal diffusivity:

$$\theta = \frac{\lambda}{\rho c} \tag{2}$$

The greater the thermal diffusivity, the shorter the time required for the material temperature transition from unsteady to steady-state.

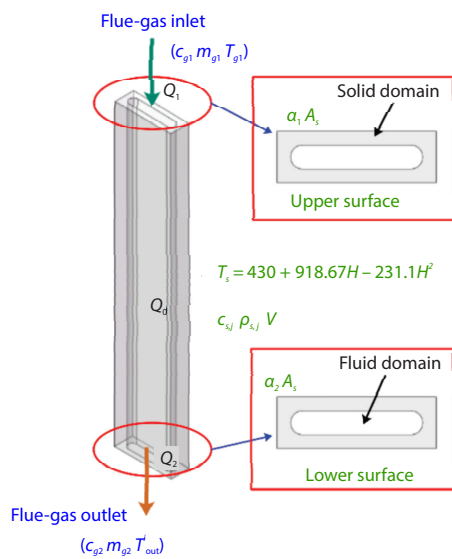


Figure 1. Thermal parameters of the fluid-solid domain of single-hole lattice brick

of the upper surface solid, Q_0 [W] was the heat absorbed by the solid material, and Q_2 [W] was the sum of the heat taken away by the flue gas and the convective heat transfer of the lower surface solid.

The each parts, fig. 1, can be expressed separately:

$$Q_1 = \alpha_1 A_s (T_{s_1}^i - T_{g_1}) + c_{g_1} m_{g_1} \Delta T_{in} \tag{3a}$$

$$Q_0 = c_{s,j} \rho_{s,j} V [T_s^i (T_{sur}^i, t) - T_s^0] \tag{3b}$$

$$Q_2 = \alpha_2 A_s (T_{s_2}^i - T_{out}^i) + c_{g_2} m_{g_2} (T_{out}^i - T_{out}^0) \tag{3c}$$

here

$$\Delta T_{in} = T_{g_1} - T_{g_0} \tag{4}$$

According to eqs. (3.1), (3.2), and (4), the TTST can be expressed:

$$T_s^i (T_{sur}^i, t) = aT_{s_1}^i + bT_{s_2}^i + cT_{out}^i + d \tag{5}$$

Total thermal storage temperature

Assuming that the temperatures of the solid domains on the XZ plane of the same Y position were equal, the sum of the temperatures of the entire solid region along the Y -direction at i minute was defined as the TTST. The TTST characterizes the total heat storage capacity of the solid material at a particular moment and evaluates the heat storage capacity of the unsteady heat transfer process. Figure 1 shows the thermal properties of inlet-outlet of flue gas and solid materials. Ignoring the radiative heat transfer of the upper and lower solid surfaces, the heat balance equation of the single-hole regenerator of the fluid-solid region at i min was established:

$$Q_1 = Q_0 + Q_2 \tag{3}$$

where Q_1 [W] was the sum of the heat absorbed by the flue gas and the convective heat transfer

Among them, the coefficients a , b , c , and d are expressed:

$$a = \frac{\alpha_1 A_s}{c_{s,j} \rho_{s,j} V} \quad (5a)$$

$$b = -\frac{\alpha_2 A_s}{c_{s,j} \rho_{s,j} V} \quad (5b)$$

$$c = \frac{\alpha_2 A_s - c_{g_2} m_{g_2}}{c_{s,j} \rho_{s,j} V} \quad (5c)$$

$$d = \frac{-\alpha_1 A_s T_{g_1} + c_{g_1} m_{g_1} \Delta T_{in} + c_{s,j} \rho_{s,j} V T_s^0 + c_{g_2} m_{g_2} T_{out}^0}{c_{s,j} \rho_{s,j} V} \quad (5d)$$

The TTST in eq. (5) is directly related to the upper and lower surface temperatures of the solid material and the flue gas outlet temperature. Equation (5) relates the flue gas outlet temperature to the heat storage capacity, and can be evaluated the thermal performance of the coke oven regenerator based on the data results.

Investigated model

Geometric model

The specific physical model of a single-hole lattice brick with the same size as the 4.3 m coke oven regenerator of a coking plant was shown in fig. 2. The high temperature smoke flowed into the lattice brick tunnel to transfer heat to the lattice bricks. The following assumptions are given to analyze and evaluate the effect of solid heat storage parameter variation on heat transfer performance:

- The physical properties of the solid material did not change with temperature.
- The inlet temperature of high temperature flue gas and flow rate were constant.
- The single-channel solid lattice brick boundary was insulated.

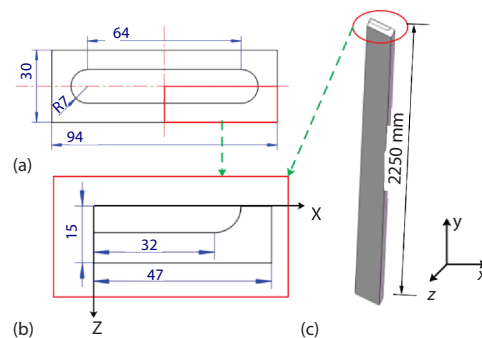


Figure 2. The simplified geometric model, A-a singlehole model, B-a quarter of the model after symmetrical treatment

Governing equations and initial conditions

This study used ANSYS FLUENT 16.0 software for numerical simulations and used its default general control equations [17]. The geometric model approximates the pipe-flow, and the calculated Reynolds number $Re < 1000$, so the Laminar flow model was used [18, 19]. The energy equation was used to simulate the flue gas-flow process [20].

The boundary conditions and the initial values of the fluid-solid region required for the simulation are shown in tab. 2.

The SIMPLE algorithm was used to solve the energy equation of the pressure field, and the second-order upwind discrete model was used to calculate the fluid-flow and heat transfer [21].

Table 2. The boundary conditions and initial values

Content	Parameter	Value
Pressure inlet boundary	Inlet pressure [Pa]	-70
	Inlet temperature [K]	1380
Pressure outlet boundary	Outlet pressure [Pa]	-77
Convective heat transfer coefficient	The upper surface [$\text{Wm}^{-2}\text{K}^{-1}$]	16.4
	The lower surface [$\text{Wm}^{-2}\text{K}^{-1}$]	9.89
Initial condition	Flue gas temperature [K]	430
	Solid temperature [K]	$*T_s = 430 + 918.67H - 231.1H^2$

* T_s is the solid domain initial temperature, and H [m] is the lattice brick height

Mesh generation and verification

We obtained a 3-D fluid-solid coupling model and an encrypted mesh according to the methods in [21]. In this example, 574426 grid elements were used for calculation.

According to the actual production condition (reversing time for 30 minutes, the coking period of 26 hours) of the on-site coke oven, the test process used three thermocouples (NWKJ-RZ, $\varnothing 20$ mm) simultaneously inserted into the measuring points 1, 2, and 3, shown as fig. 3, and the depth was 2 m. The thermocouple temperature measurement time was set to 30 hours, and the data recording used a data collector (Fluke-2638A). This paper mainly researched the thermal state changes of the solid heat storage process. Comparing the temperature results obtained from the field regenerator test and simulation found that the test results were consistent with the temperature changes of the simulation results in points 2 and 3, fig. 4. This also proved the correctness of the selected model and condition settings.

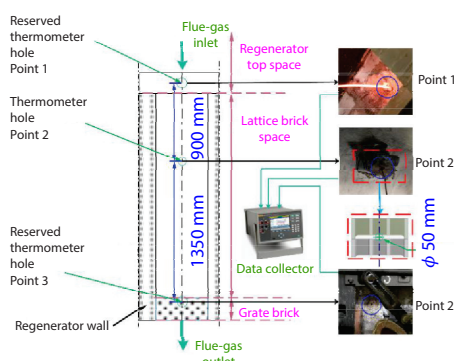


Figure 3. Distribution of temperature measuring points

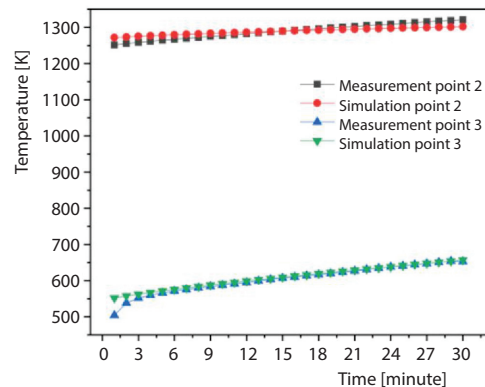


Figure 4. Temperature comparisons between numerical simulation and field test

Results and discussion

Temperature and velocity field

The different observation points, fig. 7, of Case 1, figs. 5 and 6, are selected to study the rule of unsteady heat storage during high temperature flue gas-flow. The velocity on the symmetrical boundaries of OA and OC, fig. 7(a) is the largest in the process of continuous heat storage. The high temperature flue gas passed through a flat-long lattice brick channel is

preferentially flowed through the central region by the channel resistance, resulting in a gradient distribution of velocity in the XZ plane. Influenced by the flue gas-flow characteristics, the temperature distribution in the fluid and solid domains is not uniform, fig. 6. The temperature contour variation noticeable with time presents a gradient distribution in the XZ plane at the same altitude.

From 3~30 minute, the high temperature section of the fluid region moves along the Y -direction with the temperature of solid materials gradually saturated. The solid domain temperature distribution is more complicated, which depends on convective heat transfer and heat conduction.

The solid temperature heat transfer in the OZ -direction is easier than OX -direction, fig. 7(b), and the area around point D has the lowest temperature and the slowest temperature rise. These results occur in two main ways:

- The heat transfer between the flue gas and lattice brick has periodicity and time limitation. Whether the temperature of the same height of the solid domain can satisfy the sufficient heat storage in a limited time depends on the thermal diffusion of the solid material.
- Narrow channels directly lead to the uneven distribution of air-flow, which has a significant impact on the convective heat transfer of high temperature flue-gas and solid materials. So that the temperature distribution on both sides of fig. 7(b) is unbalanced. This may be one of the reasons for the damage and cracking of lattice bricks caused by the chilling and heat shock effect caused by the periodic reversal of coke oven.

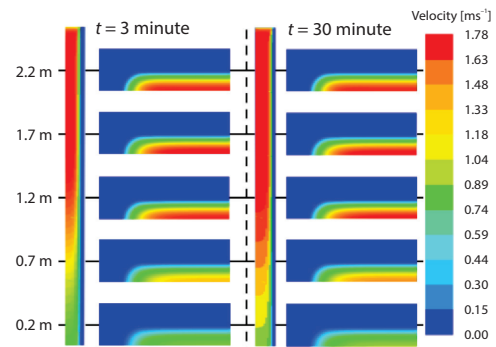


Figure 5. The contour distribution of velocity

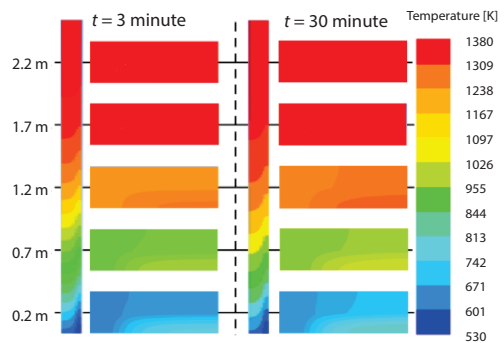


Figure 6. The contour distribution of temperature

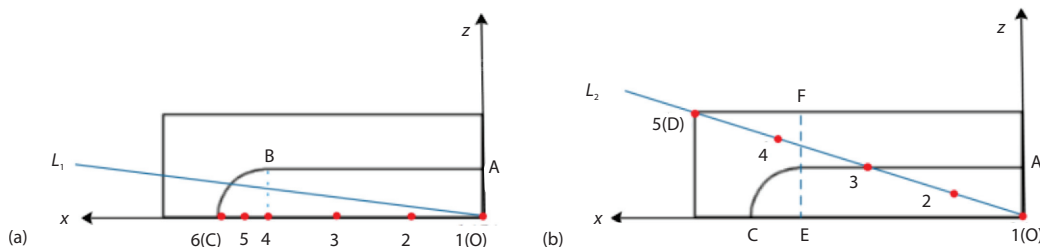


Figure 7. The distribution of observation points on the XZ plane; (a) the speed distribution of observation point and (b) the temperature distribution of observation point

It is noteworthy that although the corresponding velocity at Points 1-6 does not change significantly with the increase of heat storage time in fig. 8. However, each time point shows that the velocity distribution of the fluid field is proportional to the temperature. This is beneficial for

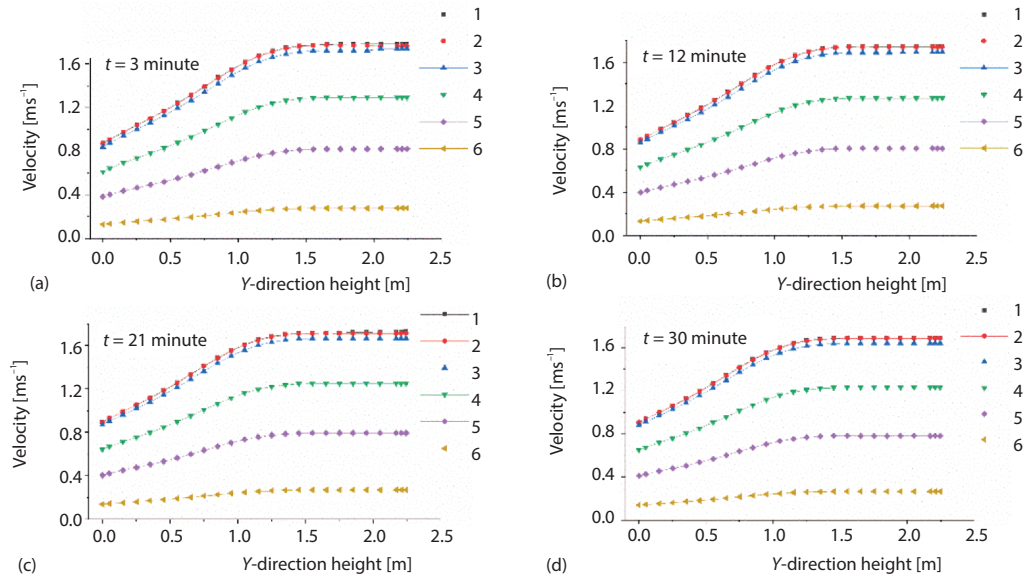


Figure 8. The speed distribution of observation points at different heights along the Y-direction with time variation

the coupling technology of heat storage and SNCR denitrification. The optimum temperature range for SNCR denitrification is about 1100~1300 K. Lower flow rate is beneficial to the full mixing reaction of flue gas and reducing agent, thus improving the denitrification efficiency.

For further analyzing the temperature applicability of solid heat storage to SNCR denitrification, we selected observation Points 1-3 in fig. 7(b) and obtained the time-varying law of each location at different heights, fig. 8. The temperature change of observation Points 1-3 in the fluid domain is more evident than that of observation Points 3-5 in solid area at each heat storage moment. Observation Point 3 is at the junction of fluid-solid coupling, reflecting the lowest temperature of the fluid and the highest temperature of solid. Considering the requirement of SNCR denitrification, we find that the temperature of the observation Point 3 on the same *XZ* plane in the fluid domain decreases significantly in the process of 30 minutes. The lower the height of lattice brick, the higher the temperature change. At the position of 1.2 m, the temperature of observation Point 3 at 3 minutes is about 75 K compared with that of observation Point 1 at 30 minutes. To get a clearer understanding of the temperature change in the fluid field at the total height of the lattice brick, we processed the data of observation Points 1~3 and fitted the curve to obtain the eqs. (6a)-(6c).

Fitting equation of observation Point 1:

$$T_1 = 1537.48 + 1.559t - \frac{425.2}{H} + \frac{52.84}{H^2} \quad (6a)$$

Fitting equation of observation Point 2:

$$T_2 = 1541.32 + 1.676t - \frac{445.67}{H} + \frac{55.448}{H^2} \quad (6b)$$

Fitting equation of observation Point 3:

$$T_3 = 1552.658 + 1.719t - \frac{489.04}{H} + \frac{60.99}{H^2} \quad (6c)$$

Through the aforementioned equation, we can determine the time, t [minute] or the height, H , of the lattice brick and obtain the corresponding temperature. The height range corresponding to the temperature range can also be calculated according to the temperature requirement of SNCR denitrification, to determine the height unsuitable for SNCR denitrification and the space size of regenerator suitable for SNCR denitrification.

Case study on heat storage of solid materials

We combined tab. 1 to calculate the thermal effusivity and the thermal diffusivity results, tab. 3, according to eqs. (1) and (2). Table 3 shows that the increase in the specific heat, c , and density, ρ , causes the thermal effusivity to increase, which in turn increases the ability of the solid material to absorb heat. The more heat the lattice brick absorbs the flue gas, the lower the temperature of the flue gas-flowing from the bottom of the lattice brick, figs. 9(a) and 9(b). Increasing the thermal conductivity, λ , does not change the heat storage capacity of the solid material, so the outlet temperature is substantially unchanged compared to Case 1, fig. 9(c).

Table 3. The calculation results of the thermal effusivity and the thermal diffusivity

Case number	κ [Ws0.5m ⁻² K ⁻¹]	$\theta \cdot 10^7$ [m ² s ⁻¹]
Case 1	1615.12	6.25
Case 2	1688.61	5.72
Case 3	1758.98	5.27
Case 4	1826.66	4.89
Case 5	1657.11	5.94
Case 6	1698.02	5.66
Case 7	1737.98	5.40
Case 8	2156.66	11.15
Case 9	2587.21	16.05
Case 10	2955.73	20.94

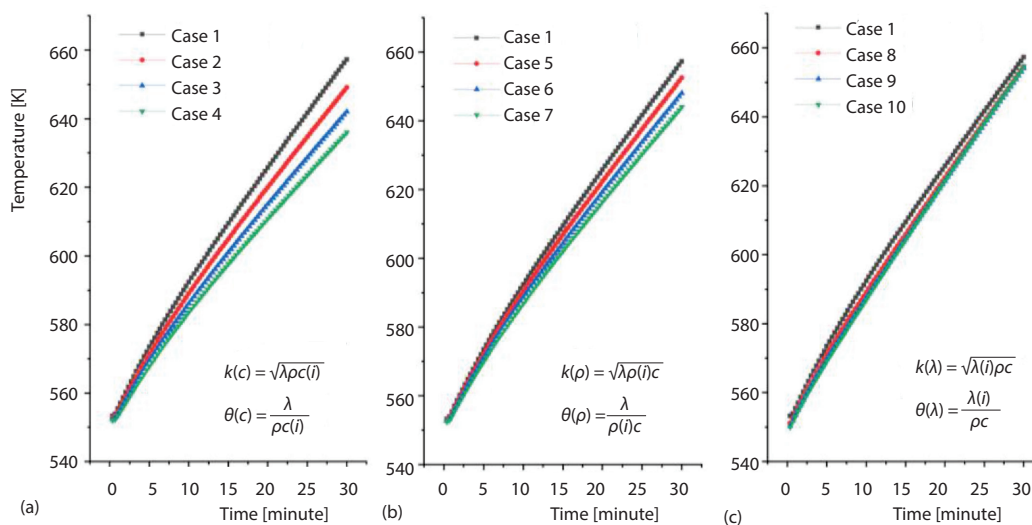


Figure 9. The outlet temperature of regenerator

Figures 10(a)-10(c) is the heat transfer power of the solid surface heat exchange of upper surface, figs. 10(d)-10(f) is the average heat transfer power of the whole single-hole lattice brick. According to 10(a)-10(d), 10(b)-10(e), a positive contribution of the thermal effusivity to heat storage is observed. While 10(c)-10(f) is consistent with fig. 10(c), it does not contribute substantially to heat storage.

From the perspective of energy balance, since the symmetry plane of the geometric model is adiabatic, the heat transferred into the regenerator through the upper surface, except for entering the solid region, the remaining portion flows out from the lower surface. The whole heat storage does not keep increasing with the increase of total heat input. However, when the regenerator is not in thermal saturation, and the outlet temperature is still within the allowable range, the total amount of heat ingress is positively correlated with the total stored heat.

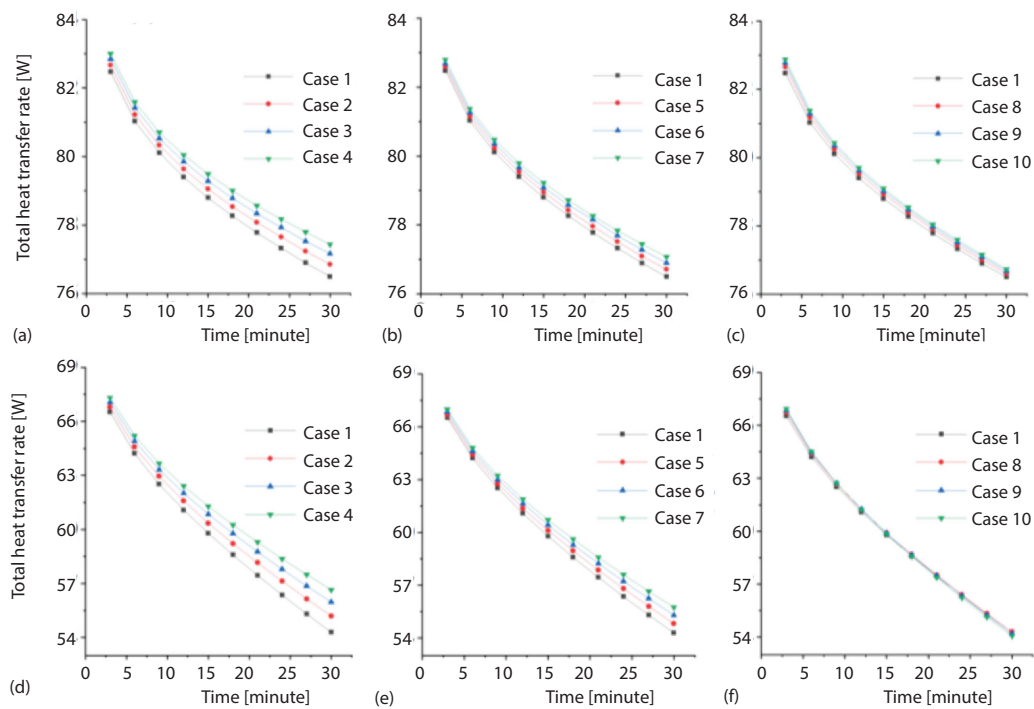


Figure 10. The heat transfer rate of heat exchange between the flue gas and lattice brick

Temperature distribution proportion

In the aforementioned, the TTST is one of the evaluation indexes of heat storage. The initial TTST T_s^0 [K] in eq. (5d) can be obtained from T_s , tab. 2 and eq. (6):

$$T_s^0 = \int_0^H T_s dh \quad (7)$$

The coefficients a , b , c , and d in eq. (5) are calculated according to the relevant parameters in tab. 4. Therefore, the TTST of eq. (5) is only related to the upper and lower solid surface temperatures as well as the flue gas outlet temperature and the heat storage time.

Table 4. Related parameters and values

Variable	Symbol	Value
Upper surface heat transfer coefficient [$\text{Wm}^{-2}\text{K}^{-1}$]	α_1	16.4
Lower surface heat transfer coefficient [$\text{Wm}^{-2}\text{K}^{-1}$]	α_2	9.89
Checker brick height [m]	H	2.25
Flue gas inlet temperature [K]	T_{g1}	1380
Flue gas inlet specific heat [$\text{Jkg}^{-1}\text{K}^{-1}$]	c_{g1}	1.27
Flue gas export specific heat [$\text{Jkg}^{-1}\text{K}^{-1}$]	c_{g2}	1.12
Flue gas initial outlet temperature [K]	T_{out}^0	430
Ambient temperature [K]	T_{g0}	273
Solid cross-sectional area [m^2]	A_s	0.0443
Flue gas-flow [kg h^{-1}]	m_{g1}	$5.8 \cdot 10^{-5}$

According to the physical property parameter $c_{s,i}$, $\rho_{s,i}$ of the Cases 1-10 material, the temperatures T_{s1}^i , T_{s2}^i , T_{out}^i corresponding to 3 minutes, 12 minutes, 21 minutes, and 30 minutes are, respectively, brought into the eq. (5) to obtain the TTST. Furthermore we define the deviation value of total thermal storage temperature (DV-TTST). The DV-TTST is the TTST compared to the reference thermal storage temperature, and its expression is shown:

$$\Delta\varepsilon = [T_s^i(T_{\text{sur}}^i, t) - \bar{T}_s^i(T_{\text{sur}}^i, t)] \cdot 10^5 \quad (8)$$

where the reference thermal storage temperature is $\bar{T}_s^i(T_{\text{sur}}^i, t) = 2414.42 \text{ K}$.

The TTST-DV was calculated according to eq. (8), shown in fig. 11. The TTST-DV indirectly reflects the total value of the thermal storage temperature obtained in the solid region over time. Figure 11(a) and 11(b) shows an increase in the thermal effusivity, and the TTST decreases. The reason is that the improvement of heat storage capacity of solids can absorb more heat, resulting in a slower temperature rise. In contrast, the increase in the thermal diffusivity of the solid material in fig. 11(c) does not affect the heat storage capacity and has no effect on the TTST.

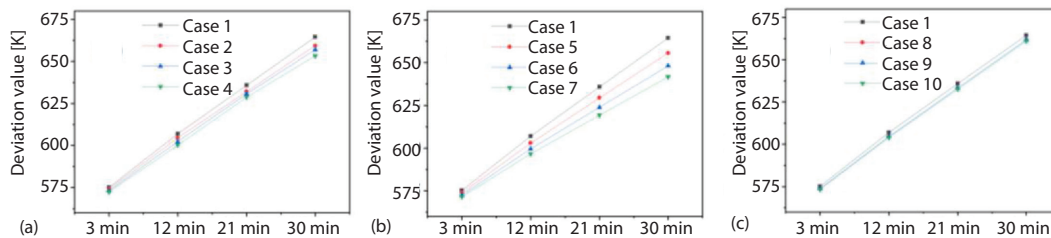


Figure 11. Variation trend of TTST deviation value

The TTST is positively correlated with the outlet temperature of flue gas. The TTST is reduced, and the corresponding flue gas outlet temperature is also reduced, reflecting the increase in heat storage. This also explains from the side that after increasing the heat storage capacity of the material, the solid heat storage temperature distribution within 30 minutes is lower

than before, and the position of the SNCR suitable denitration temperature will also increase. The specific elevated position can be determined by eq. (6).

The DV-TTST has a regular rule with the physical properties and time of the solid material. The DV-TTST under different TTST is fitted by the global algorithm:

$$\Delta\varepsilon(c) = 617.18 - 0.032\kappa(c) + 4.31t^{0.915} \quad (9a)$$

$$\Delta\varepsilon(\rho) = 671.08 - 0.063\kappa(\rho) + 4.07t^{0.911} \quad (9b)$$

$$\Delta\varepsilon(\lambda) = 585.2 - 0.013\kappa(\lambda) + 3.52t - 0.0077 \quad (9c)$$

The variation eq. (8) gives another expression:

$$T_s^i(T_{\text{sur}}^i, t) = \bar{T}_s^i(T_{\text{sur}}^i, t) + \Delta\varepsilon \cdot 10^{-5} \quad (10)$$

By changing the thermal effusivity of the solid material by the aforementioned correlation formula, it is possible to predict the TTST at different times, and further know whether the heat storage amount reaches the requirement of the preheated air.

Conclusions

The effects of physical properties of heat storage materials on the coke oven heat storage process of unsteady fluid-solid coupling coke ovens were investigated. Based on the physical properties of clay bricks commonly used in coke oven regenerators, nine sets of cases were set by changing the physical properties (specific heat, density, thermal conductivity) closely related to heat transfer. Through the simulation results of the case, the outlet temperature, heat storage capacity and the temperature space variation rule suitable for SNCR denitrification were analyzed. In addition the heat storage coefficient and the thermal conductivity as the heat storage evaluation index, the paper also proposed an index that can evaluate the unsteady heat storage process-the TTST through the heat balance analysis of the model. By analyzing the variation law of temperature field and flow field in Case 1 within 30 minutes, it was found that the flow of high temperature flue gas in the channel made the temperature transfer uneven on the *Y*-section, and the temperature gradient between the fluid and solid domain was relatively obvious. The non-uniformity of temperature distribution in the solid domain directly affected whether it meets the requirements of heat storage and the cyclic hot-cold alternating heat transfer damaged to the mechanical structure of the solid material. The relationship between temperature and time in the *Y*-height direction of the fluid domain was fitted to predict the temperature distribution of the entire fluid domain corresponding to a certain time, and the spatial distribution of the SNCR denitration temperature window was indirectly obtained. Studying the different thermal effusivity and the thermal diffusivity corresponding to the flue gas outlet temperature and heat storage, the thermal effusivity had an obvious influence on it. However, insufficient heat storage time, the thermal conductivity does not show obvious advantages. The TTST was further simplified to the DV-TTST. According to the variation rule obtained by substituting the data, it was found that the TTST is inversely proportional to the flue gas outlet temperature and proportional to the thermal storage.

Although theoretically, the thermal storage and flue gas outlet temperature can be predicted by the fitted curve. It was verified whether the actual production requirements of the coke oven can still be satisfied after changing the heat storage material, and predicted the SNCR temperature range and ammonia spray position. However, whether to achieve the coupling of heat storage and SNCR and the reduction of NO_x still need further research to confirm.

Acknowledgment

This work is financed by the National Key Research and Development Program of China under Grant No. 2017YFC0210303 and No. 2016YFB0601305.

Nomenclature

A_s – solid cross-sectional area, [m²]
 c – specific heat, [Jkg⁻¹K⁻¹]
 H – checker brick height, [m]
 m – mass-flow, [kg h⁻¹]
 T – temperature, [K]
 t – time, [min]
 V – solid volume, [m³]

Greek letters

α – convective heat transfer coefficient, [Wm⁻²K⁻¹]

ρ – density, [kgm⁻³]
 λ – thermal conductivity, [Wm⁻¹K⁻¹]

Superscripts and subscripts

i – time
in – flue gas inlet
g – flue gas
out – flue gas outlet
s – solid material
sur – solid surface

References

- [1] Zhao, B., et al., Non-Linear Relationships between Air Pollutant Emissions and PM2.5-Related Health Impacts in the Beijing-Tianjin-Hebei Region, *Sci. Total. Environ.*, 661 (2019), Apr., pp. 375-385
- [2] Yang, H., et al., The Contribution of the Beijing, Tianjin and Hebei Region's Iron and Steel Industry to Local Air Pollution in Winter, *Environ. Pollut.*, 245 (2019), Feb., pp. 1095-1106
- [3] Liu, X., et al., Emission Characteristics of Aviation Kerosene Combustion in Aero-Engine Annular Combustor with Low Temperature Plasma Assistance, *Thermal Science*, 23 (2019), 2A, pp. 647-660
- [4] Zhou, H., et al., Optimization of Ammonia Injection Grid in Hybrid Selective Non-Catalyst Reduction and Selective Catalyst Reduction System to Achieve Ultra-Low NO_x Emissions, *Journal Energy. Inst.*, 91 (2018), 6, pp. 984-996
- [5] Yu, J., et al., Sulfur Poisoning Resistant Mesoporous Mn-Base Catalyst for Low Temperature SCR of NO with NH₃, *Appl. Catal. B-Environ.*, 95 (2010), 1-2, pp. 160-168
- [6] Yu, J., et al., The Pilot Demonstration of a Honeycomb Catalyst for the DeNO_x of Low Temperature Flue Gas from an Industrial Coking Plant, *Fuel*, 219 (2018), May, pp. 37-49
- [7] Buczynski, R., et al., Investigation of the Heat-Recovery/Non-Recovery Coke oven Operation Using a 1-D Model, *Appl. Therm. Eng.*, 144 (2018), Nov., pp. 170-180
- [8] Jin, K., et al., Simulation of Transport Phenomena in Coke oven with Staging Combustion, *Appl. Therm. Eng.*, 58 (2013), 1-2, pp. 354-362
- [9] Belošević, S., et al., Modelling of Pulverized Coal Combustion for in-Furnace NO_x Reduction and Flame Control, *Thermal Science*, 21 (2017), Suppl. 3, pp. S57-S615
- [10] Hodzic, N., et al., Influence of over Fire Air System on NO_x Emissions: An Experimental Case Study, *Thermal Science*, 23 (2019), 3B, pp. 2037-2045
- [11] Gamrat, S., et al., Influence of External Flue Gas Re-Circulation on Gas Combustion in a Coke Oven Heating System, *Fuel Processing Technology*, 152 (2016), Nov., pp. 430-437
- [12] Chunming, L., *Application of Exhaust Gas Reuse Combined with SNCR Method in Denitrification of Coke Oven Gas*, Beijing University of Chemical Technology, Beijing, China, 2017
- [13] Kesong, C., Study on the Technology of Flue Gas Denitrification in Coke Oven Thermal Storage Chamber, *Shandong Metallurgy*, 38 (2016), 2, pp. 45-46
- [14] Jiandong, C., Application of Combined Desulfurization and Denitration Technology in Coke Oven Flue Gas Treatment, *Sino-Global Energy*, 23 (2018), 12, pp. 83-89
- [15] Streza, M., et al., Thermal Effusivity Investigations of Solid Materials by Using the thermal-Wave-Resonator-Cavity (TWRC) Configuration, Theory and Mathematical Simulations, *Laser Physics*, 19 (2009), 6, pp. 1340-1344
- [16] Shiming, Y., Wenquan, T., *Heat Transferology*, 4th ed., Higher Education Press, Beijing, China, 2006
- [17] ***, Fluent, I., FLUENT 6.3 User's Guide, 2006
- [18] You, Y., et al., A 3-D Numerical Model of Unsteady Flow and Heat Transfer in Ceramic Honeycomb Regenerator, *Appl. Therm. Eng.*, 108 (2016), Sept., pp. 1243-1250
- [19] Kamburova, V., et al., Numerical Modelling of the Operation of a Two-Phase Thermosyphon, *Thermal Science*, 22 (2018), Suppl. 5, pp. S1311-S1321

- [20] Yuan, F., *et al.*, Heat Transfer Performances of Honeycomb Regenerators with Square or Hexagon Cell Opening, *Appl. Therm. Eng.*, 125 (2017), Oct., pp. 790-798
- [21] Xu, Q., *et al.*, Influence of end Side Displacement Load on Stress and Deformation of L-Type Large-Diameter Buried Pipe Network, *Appl. Therm. Eng.*, 126 (2017), Nov., pp. 245-254